UNIVERSAL WISER
PUBLISHER

Research Article

Studies of Radial and Thickness Acoustic Resonance Modes of a Piezoceramic with Mixed Polarization Geometry

A. J. M. Sales[3] (iD)**, A. L. Magalhães[1]** (iD)**, R. G. M. Oliveira[1*]** (iD)**, J. E. V. de Morais[1]** (iD)**, M. A. S. Silva[1]** (iD)**, D. X. Gouveia[2]** (iD)**, D. de Andrade[4]** (iD)**, I. S. Queiroz Júnior[4]** (iD)**, A. S. B. Sombra[1,4]** (iD)

[1]Telecommunication and Materials Science and Engineering Laboratory, Physics Department, Federal University of Ceara, Fortaleza, Brazil
[2]Federal Institute of Ceara, Campus Fortaleza, Fortaleza, Brazil
[3]Physics Department, Santiago University Campus, Aveiro University, Aveiro, Portugal
[4]Federal University of Semiarid Region, Federal University of the Semi-Arid Region, Mossoró, Brazil
 E-mail: ronaldomaia@fisica.ufc.br

Abstract: In this study, the $Pb(Zr_{0.65}Ti_{0.35})O_3$ (PZT) structure was produced by the solid state reaction method, and a new polarization geometry was used to obtain the radial and thickness modes in cylindrical samples with more efficiency. The polarization procedure was investigated by varying the temperature from 30 °C to 80 °C. The experimental excitation of radial and thickness modes was observed, and a comparative study was performed with numerical simulations. The comparative analysis of the acoustic response of the cylindrical PZT samples under theoretical and experimental conditions was validated by COMSOL Multiphysics® software. The new polarization geometry technique was used to generate radial thickness and acoustic mixed modes with more efficiency. The results show that the resonance frequency and antiresonance, as well as the impedance mode and phase angle are well adjusted, showing the validation of the technique presented between the theoretical and experimental measurements.

Keywords: PZT, piezoelectric materials, mixed polarization

1. Introduction

The piezoelectric effect was discovered by Pierre and Jacques Curie in 1840, creating numerous scientific investigations relating this phenomenon to the properties of the materials, and opening possibility for a wide field of applications.[1] In the 1940s and 1950s, the study and development of piezoelectric and ferroelectric ceramics and the subsequent research of its physical properties motivated a major impetus in the development of sensors and transducers in several areas of application. Now sensors and actuators based on piezoceramics are present in a wide range of devices, such as voltage transformers, pressure sensors, audio equipment, noise and vibration control, acoustic noise suppression, sonar and fishing technology. The medical diagnosis equipment like ultrasonic images, blood pressure measurement and heartbeat monitoring, also have significantly incorporated piezoceramic technologies in the last years. The development of new techniques for use in the devices based on piezoelectric ceramics[2] needs knowledge of both the physical principles involved in the piezoelectric effect and the intrinsic properties of the materials used in a specific device design. The efforts to improve methods to obtain the constants of piezoelectric ceramics[3-6] are made and have

been carried out in recent years. New methods using the immittance spectra of the material[7, 8] are used to determine the constant stress and the constant strain.[9-12] A piece of piezo material with cylindrical circular geometry can accept permanent polarization in two ways: thickness mode and radial mode. Studies on the frequency response of these materials have reported numerical expressions for calculating the resonant frequencies in relation to the two modes mentioned (thickness mode and radial mode).[2]

In this work, we studied the $Pb(Zr_{0.65}Ti_{0.35})O_3$ (PZT) compound (herein named PZT10) manufactured in a circular cylindrical geometry.[13] The two modes (thickness and radial) and a new polarization strategy are studied. First the frequency response was obtained separately for each mode (thickness and radial) using the theoretical expressions in the mentioned literature. Then a numerical procedure based on the COMSOL Multiphysics® software was used to study the resonance regions for both modes, through numerical simulation. Finally, we proposed a new form of polarization (described in Section 2.3) combining the two modes, in order to verify how a new spatial distribution of the permanent dipoles influences the resonant frequencies modes and investigate the possibility of exciting a combination of thickness and radial modes. This new form of polarization is referred in our work as "mixed polarization geometry".

2. Theory

The traditional methods to setup a permanent polarization in a cylindrical sample of piezoelectric material are the radial polarization and the thickness polarization. When the radial form of polarization is chosen, the resonant frequencies associated with this polarization strategy are at lower frequency ranges. (considering that the diameter is much bigger than the thickness). Otherwise, for the thickness polarization, the resonant frequencies are at higher range of frequencies.[5,6] The values of the resonance frequencies for the two modes are investigated to obtain a computational model that indicates the resonance and antiresonance frequencies.[9, 10] The characterisation of lossy piezoelectric materials in the PZT case, can be done through both cases-the investigation of resonant frequencies in the thickness or radial modes by examining the complex impedances Z (or admittances Y) versus frequency of the PZT (frequency response).[9] The methods used to determine the material constants, in the complex form, are iterative[14] and non-iterative.[15]

2.1 *Radial mode*

To determine the material piezoelectric constants in complex form, interactive[7, 8, 14] and non-interactive[15, 16] methods are used. In the interactive method, the frequency spectrum of the electrical admittance is used within the range of the resonance-antiresonance of the fundamental mode.[9] To determine the dielectric constants at constant stress or strain, the non-iterative methods are used away from the fundamental resonance,[9] so that this method can be used in the radial mode when the material has intermediate mechanical quality factors.[15]

The method used for the radial mode measurements, through admittance (Y), obeys Equation (1),[8] relating admittance versus frequency as follows:

$$Y = i\frac{2\pi^2 f a^2}{t}\left[\varepsilon_{33}^T + 2d_{31}^2 \frac{c_{11}^p}{\cfrac{1}{2 - ji\left[2\pi fa\sqrt{\dfrac{\rho}{c_{11}^p}}\right]} - \cfrac{1}{1+\sigma}}\right] \tag{1}$$

where f, a, t and ρ are the resonance frequency, radius, thickness and density of the sample, respectively and $i = \sqrt{-1}$ and ji condition of radial resonance in a lossless piezoceramic resonator with all material constants as real quantities. The piezoelectric constant d_{31}, the dielectric permittivity ε_{33}^T, elastic constant c_{11}^p and Poisson's ratio σ are complex quantities represented by Equations (2) and (3).

$$c_{11}^P = \frac{s_{11}^E}{\left(s_{11}^E\right)^2 - \left(s_{12}^E\right)^2} \tag{2}$$

$$\sigma = -\frac{s_{12}^E}{s_{11}^E} \tag{3}$$

where s_{11}^E and s_{12}^E are defined with the elastic compliances at constant field E.

2.2 Thickness mode

The model developed for radial mode can be extended for the thickness mode by examining the impedance Z.[9] The electrical impedance Z versus frequency f (frequency response) is given by Equation (4).

$$Z = i\frac{t}{2\pi f A \varepsilon_{33}^S} + i\frac{h_{33}^2 tan\left(\pi ft\sqrt{\frac{\rho}{c_{33}^D}}\right)}{2\pi^2 A f^2 c_{33}^D \sqrt{\frac{\rho}{c_{33}^D}}} \tag{4}$$

where A, t and ρ are the electrode area, thickness and density of the sample, respectively and $i = \sqrt{-1}$. The piezoelectric constant h_{33}, the dielectric permittivity at constant strain ε_{33}^S and the elastic stiffness at constant dielectric displacement c_{33}^D are complex quantities, which are performed by an iterative process that requires initial estimation of the elastic constant,[10] represented by Equation (5).

$$c_{33}^D = 4\rho t^2 f_P^2 \left[1 + i\frac{f_{Xmin} - f_{Xmax}}{f_P}\right] \tag{5}$$

With this initial estimation of c_{33}^D, the electrical impedance determined by Equation (4) becomes linear in $\frac{1}{\varepsilon_{33}^S}$ and h_{33}^2. One step in the iteration process is complete when the cut criterion is met, as shown in Equation (6).

$$\frac{\left|c_{33f}^D - c_{33i}^D\right|}{\left|c_{33f}^D\right|} \leq 10^{-8} \tag{6}$$

The subscripts i and f correspond to the initial and final values of c_{33}^D in an iteration step.

2.3 Mixed polarization

In this study, the term mixed polarization is used to describe the result of applying the high polarization voltage between the external electrodes with different radii (see Figure 3b). It is expected that the E field during the process of polarization has two preferred directions. Looking at the cylindrical part (see Figure 3b) is expected that E to have a direction parallel to the z-axis (i.e., along the disc thickness), and another radial, along to the radius r of the cylinder. Therefore, it is expected that the resulting permanent polarization will be a combination of thickness and radial modes.

2.4 Simulation using COMSOL Multiphysics® software

To validate the experimental results, computational simulations based on finite element method were performed using the COMSOL Multiphysics® software. The piezoelectric ceramic was designed by using a cylindrical geometry in which two electrodes were applied on its upper and lower surfaces. In this model, the polarization was adopted on the

thickness direction. The radius a is 11.27 mm and the height h is 0.98 mm. The piezoelectric parameters of the PZT4 material were adopted to start the simulations. The PZT4 density ρ is 7500 kg/m^3 and the compliance, coupling and relative permittivity matrices are given by Equations (7), (8) and (9).

$$s^E = \begin{bmatrix} 12.3 & -4.05 & -5.31 & 0 & 0 & 0 \\ 0 & 12.3 & -5.31 & 0 & 0 & 0 \\ 0 & 0 & 15.5 & 0 & 0 & 0 \\ 0 & 0 & 0 & 39 & 0 & 0 \\ 0 & 0 & 0 & 0 & 39 & 0 \\ 0 & 0 & 0 & 0 & 0 & 32.7 \end{bmatrix} 10^{-12} \ 1/\text{Pa} \tag{7}$$

$$d = \begin{bmatrix} 0 & 0 & 0 & 0 & 4.96 & 0 \\ 0 & 0 & 0 & 4.96 & 0 & 0 \\ -1.23 & -1.23 & 2.89 & 0 & 0 & 0 \end{bmatrix} 10^{-10} \ \text{C/N} \tag{8}$$

$$\varepsilon_r^T = \begin{bmatrix} 1475 & 0 & 0 \\ 0 & 1475 & 0 \\ 0 & 0 & 1300 \end{bmatrix} \tag{9}$$

The values of ρ and d_{31}^T were changed to match with experimental radial mode, and their values at the end of the simulations were $\rho = 7900$ kg/m^3 and $d_{31}^T = 1.3 \times 10^{-10}$ C/N. The thickness mode remained unchanged with such modification.

2.5 *Simulation using SCILAB*

According to some other studies,[9,10] the electrical admittance Y, as a function of the frequency f of a thin ceramic disk, polarized in the thickness direction and vibrating in the radial mode, can be determined from Equation (10).

$$Y = i \frac{2\pi^2 f a^2}{h} \left[\varepsilon_{33}^T + 2d_{31}^2 \frac{c_{11}^P}{\dfrac{1}{2 - \Im_1(z)\left[2\pi f a \sqrt{\rho / c_{11}^P}\right]} - \dfrac{1}{1+\sigma}} \right] \tag{10}$$

where $i = \sqrt{-1}$ and the dielectric permitivity at constant stress ε_{33}^T is given by $\varepsilon_{r33}^T \varepsilon_0$. The Poisson's ratio σ and the elastic constant c_{11}^P are given by Equations (2), (3) and $\Im_1$ is a complex function called Onoe's function by Meitzler et al.[11], and is defined by Equation (11).

$$\Im_1(z) = \frac{z J_0(z)}{J_1(z)} \tag{11}$$

where J_0 and J_1 are Bessel functions of the first kind of zero and first orders of the complex variable z, given by Equation (12).

$$z = 2\pi f a \sqrt{\rho / c_{11}^P} \tag{12}$$

Finally, the electrical impedance can be obtained from $Z = 1/Y$. The electrical impedance Z, as a function of the frequency f for such disk, vibrating in the thickness mode, can be determined from Equation (13).[11]

$$Z = -i\frac{t}{2\pi fA\varepsilon_{33}^{S}} + i\frac{h_{33}^{2}\tan\left(\pi ft\sqrt{\rho/c_{33}^{D}}\right)}{2\pi^{2}Af^{2}c_{33}^{D}\sqrt{\rho/c_{33}^{D}}} \tag{13}$$

where A is the electrode area, the dielectric permittivity at constant strain ε_{33}^{S} is given by $\varepsilon_{r33}^{S}\varepsilon_{0}$. The piezoelectric constant h_{33} and the elastic stiffness at constant dielectric displacement c_{33}^{D} are given by Equations (14) and (15).

$$h_{33} = \frac{e_{33}}{\varepsilon_{33}^{S}} \tag{14}$$

$$c_{33}^{D} = c_{33}^{E} + h_{33}^{2}\varepsilon_{33}^{S} \tag{15}$$

3. Experimental procedure

The synthesis of phase PZT powder was prepared by means of a conventional solid-state reaction method[13] in which stoichiometric mixtures of metallic oxides were used, according to Equation (16), with commercially available PbO, ZrO$_2$ and TiO$_2$, all of them having the Aldrich mark of high purity (> 99%).

$$PbO + 0.65ZrO_2 + 0.35TiO_2 = Pb(Zr_{0.65}Ti_{0.35})O_3 \tag{16}$$
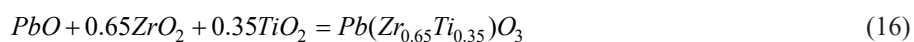
In the grinding process, the mixture was placed inside the polyacetal reactors, whose approximate volume is 221.69 cm^3, containing approximately 98 g of zirconia beads per 10 g of reagents. In this process, the elimination of aggregates and/or reduction of particle size needs activation energy, so that the energy required in the reaction of the phase synthesis in the calcination process is lower. The sealed casings were placed in a Fritsch Pulverissette 6 planetary mill, and the high energy mechanical milling was performed for 1 h.

The powder resulting from the mechanical milling was transferred to an alumina crucible and brought to the resistive kiln of the brand "Jung" model LF0912 to undergo calcination, which was carried out at 850 °C for 2 h for the formation of PZT, with a heating and cooling rate of 5 °C/min. The powders were subsequently examined at room temperature by X-Ray diffraction (XRD), using Cokα radiation with wavelength ($\lambda = 0.178896$ ηm), over an angular range of ($20° \leq \theta \leq 80°$) and a sweeping rate of $0.5°$ min^{-1}, in lead atmosphere to avoid the lead loss in relation to PZT.

To identify the formed phases, the quantitative analysis of the Rietveld method was used. The peaks, shown in Figure 1, were identified with the reference standard inorganic crystal structure database (ICSD) 86136. The parameters, such as quality factor (S), residual error (R-Wp), Bragg-R-factor, and theoretical density, are presented in Table 1.[17] The PZT has a high relative density (98%), which is in agreement with the values found in the literature.[18, 19]

Table 1. The PZT lattice parameters and agreement parameters obtained from Rietveld method

a (Å)	b (Å)	c (Å)	α (°)	β (°)	γ (°)
5.7826	5.7826	14.2723	90	90	120

Theorical density (g/cm³)	S	Bragg-R-factor	R-Wp	R-P	R-expected
7.97	1.67	3.14	6.62	4.66	3.894
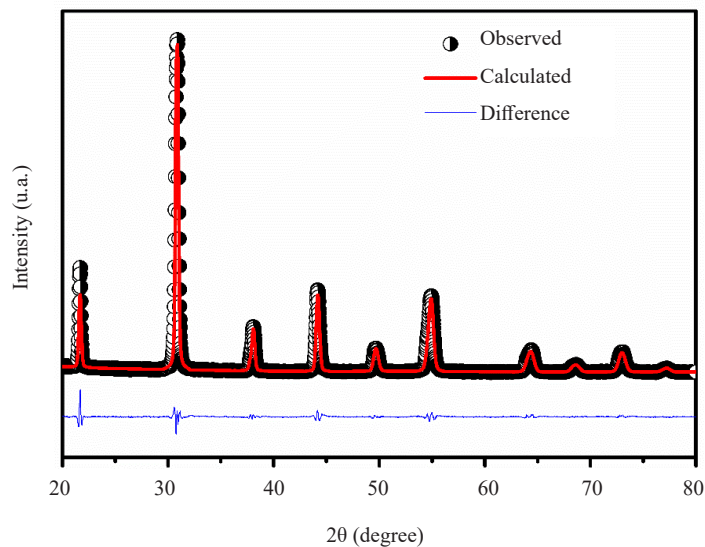
Figure 1. Observed and calculated intensity of the powder diffraction pattern of PZT

The cylinder was produced by pressing the powder uniaxially in a steel mold at 100 MPa, and then statically pressed at 600 MPa and sintered at 1150 °C under a 3% lead atmosphere for 2 h, at a rate of 5 °C/min.
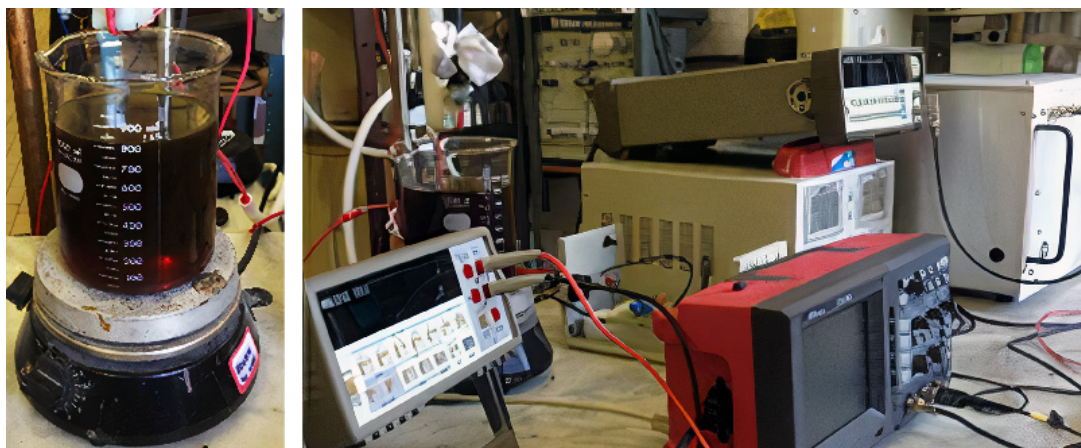
Figure 2. Mixed polarization system

The process of polarization-radial and thickness-were performed simultaneously varying the temperature from 30 °C to 80 °C, by using manufactured by TREK model 20/20C High Voltage Amplifier for 1 h, under the polarization voltage of 3000 V, according to the system shown in Figure 2.
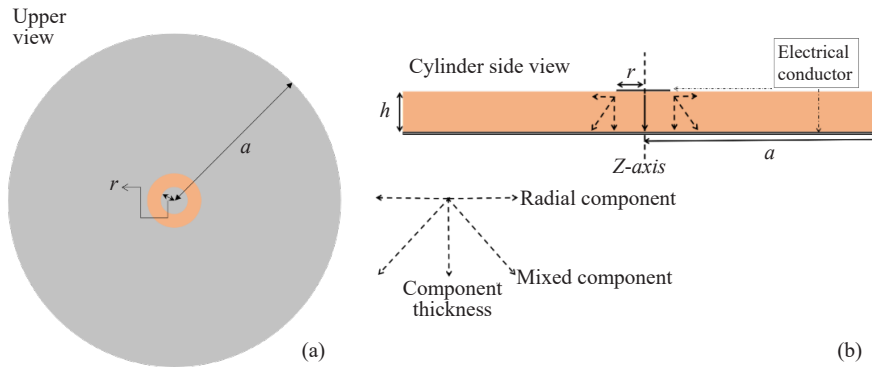
Figure 3. (a) PZT sample prototype and (b) projection of the electrodes in the PZT sample for polarization

The sample of PZT that was polarized (Figure 3a), has an external radius (a) of 11.27 mm, height h = 0.98 mm and internal electrode radius (r) = 2.08 mm, and its projected configuration is shown in Figure 3b.

4. Results and discussions

The measurement technique applied to the cylindrical sample electrodes produces a sinusoidal voltage stimulation and performing a frequency sweep, by means of an HP4194A (0 to 110 MHz) impedance gain/phase analyser, controlled by a computer. According to the theory, the sample will display a frequency response, where resonance and antiresonance frequencies can be investigated in a large range of frequencies. In this work, using SCILAB, we numerically calculate the impedance (admittance) of the acoustic resonator by adopting Equation (1) (radial mode), and Equation (4) (thickness mode) and also using COMSOL Multiphysics® software, we did the same analysis for the same modes. In Figures 4 and 5, we did a comparison of the simulations (SCILAB and COMSOL Multiphysics® software numerical techniques) with the experimental data. SCILAB is an open scientific software for numerical computing similar to MATLAB that provides a powerful computing environment for scientific applications. COMSOL Multiphysics® software is a finite element platform analysis, solver and simulation software. It allows conventional physics-based user interfaces and coupled systems of partial differential equations.

Figure 4 shows a curve generated by SCILAB, which simulates Equation (15), and also shows a curve generated by COMSOL Multiphysics® software, considering the PZT characteristics required by the software. It can be observed that the resonant and anti-resonant frequencies attributed to the radial mode are at 99 kHz and 117 kHz with a bandwidth of 18 kHz. The experimental resonance is around 107 kHz with lower bandwidth (around 2 kHz) compared to the simulated results. Both curves agree with the experimental results, validating the results indicated by the simulation. In Figure 4(a, b) and Figure 5(a, b), the Impedance Z and Theta = arctg(Im{Z}/Re{Z}), was obtained thorough SCILAB and COMSOL Multiphysics® software numerical techniques.

According to Figure 5, the simulation curves (SCILAB and COMSOL Multiphysics® software) also agree with the experimental results, so when polarizing with the mixed polarization, the frequency of 2 MHz is attributed to the presence of the thickness component.

The impedance modulus at these frequencies is 4.12 Ω and 17.86 kΩ, respectively. The resonant and anti-resonant frequencies attributed to the thickness mode are 2 MHz and 2.24 MHz with a bandwidth of 240 kHz. The impedance modulus at these frequencies is 2.12 Ω and 303.41 Ω, respectively. The experimental resonance is around 2.110 MHz with a lower bandwidth (around 30 kHz) compared to the simulated results. The bandwidth is lower compared to the numerical results.

Figure 4c and Figure 5c are results from the COMSOL Multiphysics® software simulation, indicating the vibrations resulting from the mechanical stress and the presence of radial and thickness vibrations.
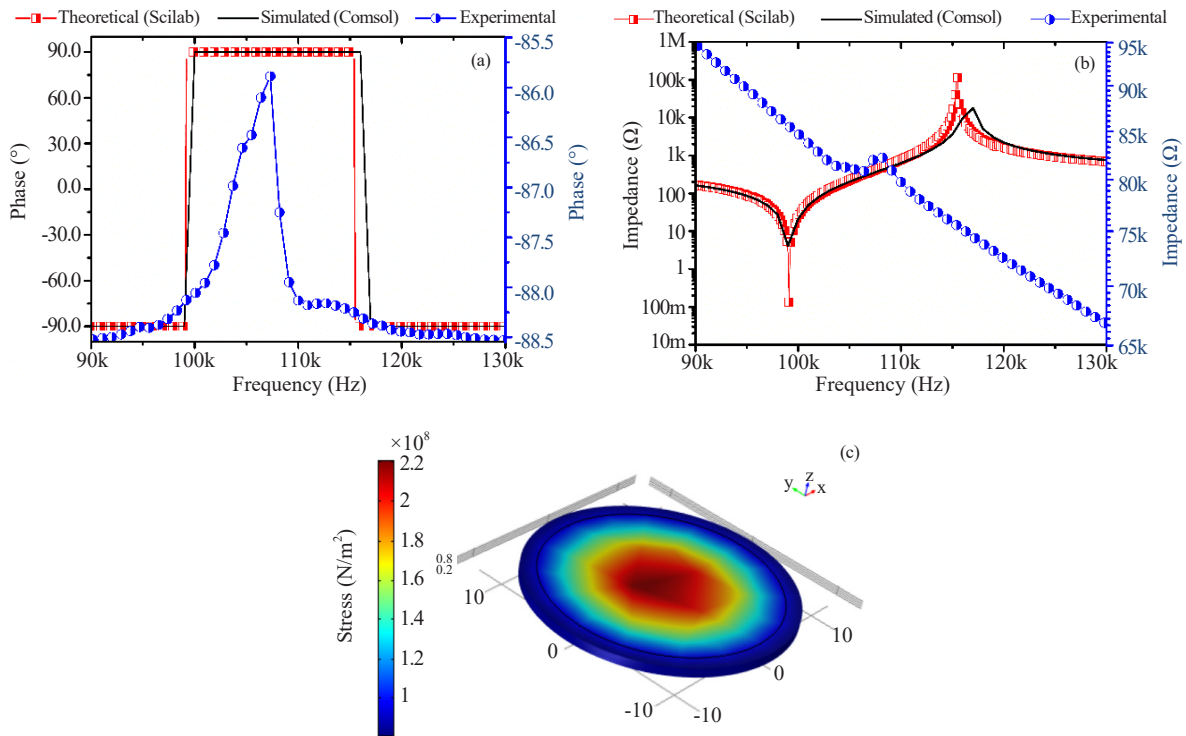
Figure 4. Theoretical simulated and measured results of the impedance modulus resonance and phase angle of the radial mode: (a) Phase, (b) Impedance and (c) Simulation of stress contour plot due to radial mode (COMSOL Multiphysics® software)
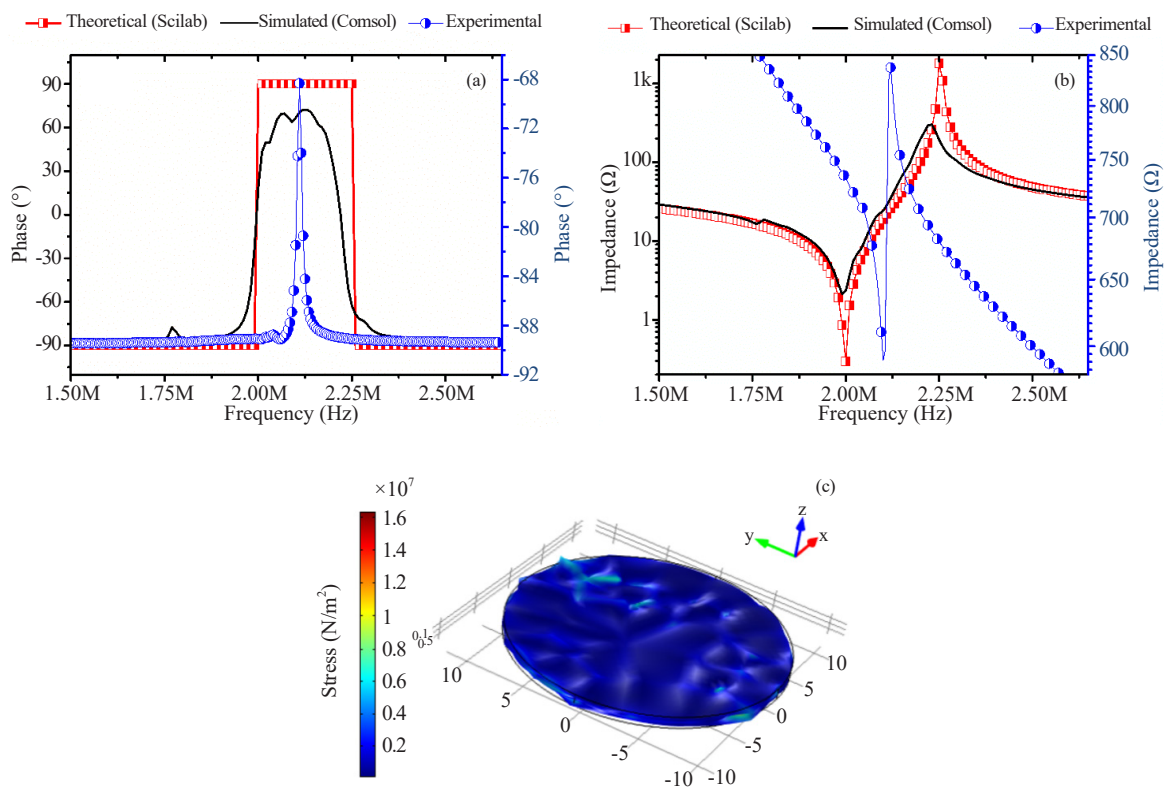
Figure 5. Theoretical simulated and measured results of the phase mode impedance and resonance modulus of the thickness mode. (a) Phase, (b) Impedance and (c) Simulation of mechanical deformation due to thickness mode (COMSOL Multiphysics® software)

5. Conclusions

A cylindrical resonator was manufactured from PZT. The crystal phase was confirmed by XRD analysis, and the parameters for refinement by the Rietveld method showed the formation of the PZT structure. The experimental results of the characterisation of a new mixed polarization geometry were applied for a PZT sample to control the thickness and radial configuration simultaneously with good efficiency. Moreover, the theoretical results (obtained by simulations) for resonance and antiresonance of a sample of the same material and same dimensions with thickness bias, were presented in thickness and radial modes. The simulated results of the impedance modulus and phase angle were quite adjusted in relation to the frequency and bandwidth and were quite consistent with the experimental data, showing that with the mixed polarization geometry both the modes radial and thickness are present.

Conflict of interest

The authors declare no competing financial interest.

References

[1] Chamankar, N.; Khajavi, R.; Yousefi, A. A.; Rashidi, A.; Golestanifard, F. *Ceram. Int.* **2020,** *46*, 19669.

[2] Moheimani, S. O. R.; Fleming, A. J. *Piezoelectric Transducers for Vibration Control and Damping*; Springer, 2006.

[3] Qiao, L.; Li, G.; Tao, H.; Wu, J.; Xu, Z.; Li, F. *Ceram. Int.* **2020,** *46*, 5641.

[4] Amarande, L. *J. Eur. Ceram. Soc.* **2014,** *34*, 1547.

[5] Amarande, L. *J. Eur. Ceram. Soc.* **2012,** *32*, 1099.

[6] Masaki, M.; Hashimoto, H.; Masahiko, W.; Suzuki, I. *J. Eur. Ceram. Soc.* **2008,** *28*, 133.

[7] Alemany, C.; Pardo, L.; Jimenez, B.; Carmona, F.; Mendiola, J.; Gonzalez, A. M. *J. Phys. D. Appl. Phys.* **1994,** *27*, 148.

[8] Alemany, C.; Gonzalez, A. M.; Pardo, L.; Jimenez, B.; Carmona, F.; Mendiola, J. *J. Phys. D. Appl. Phys.* **1995,** *28*, 945.

[9] Amarande, L.; Miclea, C.; Tanasoiu, C. *J. Eur. Ceram. Soc.* **2002,** *22*, 1873.

[10] Amarande, L.; Miclea, C.; Tanasoiu, C. *J. Eur. Ceram. Soc.* **2003,** *23*, 1139.

[11] Heywang, W.; Lubitz, K.; Wersing, W. *Piezoelectricity: Evolution and Future of a Technology*; Springer Series In Materials Science: Berlin, 2008.

[12] Jiashi, Y. *Piezoelectric Transducers for Vibration Control and Damping*; Springer, 2006.

[13] Du, W.; Hoyt, J.; Williams, N.; Cook-Chennault, K. A. *J. Manuf. Process.* **2020,** *57*, 48.

[14] Smits, J. G. *IEEE Trans. Sonics Ultrason.* **1976,** *23*, 393.

[15] Sherrit, S.; Gauthier, N.; Wiederick, H. D.; Mukherjee, B. K. *Ferroelectrics* **1991,** *119*, 17.

[16] Sherrit, S.; Wiederick, H. D.; Mukherjee, B. K. *Ferroelectrics* **1992,** *134*, 111.

[17] Rietveld, H. M. *Acta Crystallogr.* **1967,** *22*, 151.

[18] Li, W.; Liu, T.; Zou, D.; Wang, J.; Yi, T. *Mech. Syst. Signal Process.* **2019,** *129*, 455.

[19] Promsawat, M.; Watcharapasorn, A.; Sreesattabud, T.; Jiansirisomboon, S. *Ferroelectrics* **2009,** *382*, 166.